Corrosion Science 84 (2014) 66–73

Contents lists available at ScienceDirect

Corrosion Science

journal homepage: www.elsevier.com/locate/corsci

One-step formation and photocatalytic performance of spindle-like TiO_2 nanorods synthesized by dealloying amorphous $Cu_{50}Ti_{50}$ alloy

Zhengfeng Zhao [a,b], Jing Xu [a], Peter K. Liaw [c], Bo Wu [a], Yan Wang [a,b,*]

[a] School of Materials Science and Engineering, University of Jinan, No. 336, West Road of Nan Xinzhuang, Jinan 250022, PR China
[b] Shandong Provincial Key Laboratory of Preparation and Measurement of Building Materials, University of Jinan, No. 336, West Road of Nan Xinzhuang, Jinan 250022, PR China
[c] Department of Materials Science and Engineering, University of Tennessee, Knoxville, TN, USA

ARTICLE INFO

Article history:
Received 30 December 2013
Accepted 6 March 2014
Available online 11 March 2014

Keywords:
A. Copper
A. Titanium
B. SEM
C. De-alloying
C. Amorphous structures
C. Acid corrosion

ABSTRACT

The dealloying process of amorphous $Cu_{50}Ti_{50}$ powders and the formation of spindle-like rutile TiO_2 nanorods have been investigated. The amorphous $Cu_{50}Ti_{50}$ powders were prepared by a mechanical alloying method. The results show that the rutile TiO_2 nanostructures can be facilely obtained through the one-step dealloying of amorphous $Cu_{50}Ti_{50}$ powders in a concentrated HNO_3 solution. The as-dealloyed powders exhibit a "core–shell" structure after the short-term dealloying treatment. Both discrete TiO_2 nanorod shells and nanoflower clusters are formed after the long-term dealloying. In addition, the as-obtained TiO_2 nanorods exhibit a good photocatalytic performance for the degradation of methyl orange.

1. Introduction

It is well-known that TiO_2 has been widely employed for photocatalytic applications because of its cheapness, non-toxicity, and stability [1,2]. Generally, TiO_2 exists in three kinds of phases: brookite, anatase, and rutile. In contrast with the other two phases, rutile TiO_2 is the most stable phase even in strongly acidic or basic solutions. Rutile TiO_2 has been extensively used in lithium ion batteries [3,4] and dye-sensitized solar cells [5]. However, rutile TiO_2 receives little attention in the photocatalytic degradation of organic pollutants, such as colorants. Recently, it has been reported that rutile TiO_2 with different morphologies showed the efficient photocatalytic activity in photo-oxidation of organic pollutants under ultraviolet light or artificial solar light irradiation [6–10]. At present, several methods have been developed to prepare TiO_2, such as structural templates [11], metal–organic chemical vapor deposition [12], high-temperature post annealing processes [13], sol–gel method [14] and hydrothermal synthesis [15], and so forth. Moreover, various attempts have been made to improve the efficiency and use of TiO_2 in more widespread applications, such as impurity doping [16,17], noble metal deposition [18–20], and surface fluorination [21–23].

Most recently, the dealloying strategy has been explored to fabricate nanostructured oxides [24–26]. Dealloying refers to the selective removal of one element from an alloy. This method has attracted considerable attention due to its advantage for the rapid and straightforward fabrication of functional nanostructured materials [27], and has been widely utilized to fabricate nanoporous metals [28–30], nanoporous alloys [31,32], and metal oxides [26,33,34]. Compared to crystalline alloys (solid solutions and intermetallic compounds), however, less attention has been paid to the dealloying of amorphous alloys. Amorphous alloys are considered as good precursors for dealloying due to their metastable state, microstructure down to subnanoscale [35] and monolithic phase with a homogeneous composition [36,37]. Recently, studies have been conducted on the dealloying behavior of amorphous alloys. Wang and coworkers [38] have fabricated a novel Zr-doped titanate nanobelt material by dealloying Ti-based amorphous powders. Aburada and coworkers [36] have not only fabricated nanoporous copper by dealloying Al–Cu–Mg amorphous alloys, and further explored the effect of minor Ni addition. Luo et al. [37] have synthesized nanoporous copper by electrochemical dealloying of $Mg_{90-x}Cu_xY_{10}$ glassy precursors in the H_2SO_4 aqueous solution.

In the present study, amorphous $Cu_{50}Ti_{50}$ powders were successfully prepared by a mechanical alloying (MA) method and utilized as the precursor alloy for dealloying. In addition, it is necessary to point out that the $Cu_{50}Ti_{50}$ amorphous alloy with an equal atomic ratio is an interesting system for the study on its crystallization behavior [39], elastic property [40], and corrosion behavior

* Corresponding author at: School of Materials Science and Engineering, University of Jinan, No. 336, West Road of Nan Xinzhuang, Jinan 250022, PR China. Tel.: 86 531 82765473; fax: 86 531 87974453.
E-mail address: mse_wangy@ujn.edu.cn (Y. Wang).

http://dx.doi.org/10.1016/j.corsci.2014.03.014
0010-938X/

[41]. In the previous work, we have prepared $Cu_{50}Ti_{50}$ amorphous powders using the MA method [42]. The aim of the present work is to detailedly study the microstructural evolution of the amorphous $Cu_{50}Ti_{50}$ powders and the formation of spindle-like TiO_2 nanorods during the dealloying process in a HNO_3 solution. The microstructure and photocatalytic performance of the as-synthesized TiO_2 nanorods have also been investigated. This work can provide a new strategy for the facile fabrication of TiO_2 nanomaterials through dealloying of amorphous powders.

2. Experimental

Powder mixtures of elemental Ti (<70 μm, 99.5 wt.% purity) and Cu (<70 μm, 99.9 wt.% purity) with a nominal composition of $Cu_{50}Ti_{50}$ were mechanically alloyed in a high-energy ball mill (Fritsch P6) at a rotation speed of 300 rpm (revolutions per minute). The chromium steel vial and balls were used in the present work. MA was carried out at room temperature in an Ar atmosphere with a ball-to-powder weight ratio of 17:1. In order to avoid an increase in the vial temperature, the milling procedure was interrupted every 0.5 h and then halted for another 0.5 h. In addition, the milling process was interrupted at various time intervals in order to remove small amounts of the as-milled products for analysis and characterization. The phase constitution of the as-milled $Cu_{50}Ti_{50}$ powders was examined by X-ray diffraction (XRD) using Cu Kα radiation. Thermal analysis of the as-milled samples was performed on a differential scanning calorimeter (DSC) at a heating rate of 20 K/min.

The as-milled amorphous powders with a mass of 0.5 g were immersed in a HNO_3 solution with a concentration of 13.14 mol/L for different dealloying durations under free corrosion conditions. In order to promote the dealloying process, the reaction temperature was controlled at 343 K in a water bath. The as-dealloyed samples were washed using deionized water and ethanol for several times in order to remove the residual chemical substances. The microstructures of the as-dealloyed products were investigated by XRD, field-emission scanning electron microscopy (FESEM) coupled with energy dispersive spectroscopy (EDS), and transmission electron microscopy (TEM) coupled with selected area electron diffraction (SAED).

The photocatalytic performance of the as-dealloyed samples was evaluated by the photodegradation of methyl orange using a 250 W high-voltage mercury lamp with ultraviolet (UV) light. TiO_2 powders with a mass of 0.01 g were dispersed in a 100 mL methyl orange solution with a concentration of 20 mg/L, and the solution was stirred in the dark for 20 min to achieve adsorption saturation. Then the irradiation lasted in the dark for 60, 120, 180, 240 and 300 min for the photodegradation of methyl orange. The solution concentration was determined by a UV-3200 spectrophotometer at 464 nm, which is the maximum absorbance wavelength of methyl orange. The photodegradation efficiency, given as a percentage, refers to the difference in the concentration of methyl orange solution before irradiation (C_0) and after light irradiation for M (M = 60, 120, 180, 240 and 300) min (C_M) divided by C_0 (i.e., $100[C_0 - C_M]/C_0$).

3. Results and discussion

Fig. 1a shows the XRD patterns of the as-milled $Cu_{50}Ti_{50}$ powders after the selected MA time. At the early stage of ball milling (10 h), the sample is just a polycrystalline mixture of starting reactant powders, as indicated by sharp Bragg-peaks corresponding to the elemental Cu and Ti (Fig. 1a). After 20 h of MA, all the Bragg-peaks corresponding to the unprocessed elemental powders disappear and a pronounced smooth hump appears at $35° < 2\theta < 50°$,

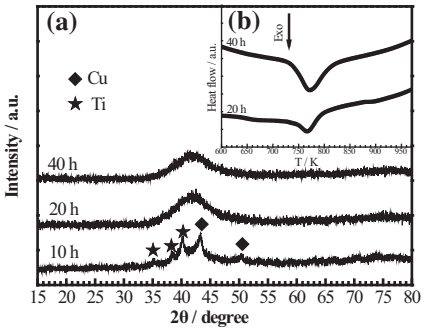

Fig. 1. XRD patterns (a) of the as-milled $Cu_{50}Ti_{50}$ powders after different MA time and DSC traces (b) of the as-milled $Cu_{50}Ti_{50}$ powders after 20 and 40 h of the MA time at the heating rate of 20 K/min.

implying the formation of a single amorphous phase (Fig. 1b). In order to obtain the smaller particles of the $Cu_{50}Ti_{50}$ amorphous phase, the powders were continuously milled up to 40 h under the same ball-milling conditions. With increasing the milling time to 40 h, it can be seen from Fig. 1a that the as-milled product is still a single amorphous phase. This trend demonstrates that no mechanically induced crystallization occurs during the prolonging milling process, and the extended milling just broke the $Cu_{50}Ti_{50}$ amorphous phase into smaller particles. In order to further confirm the amorphous structure, the as-milled samples were examined using DSC. Fig. 1b shows the DSC traces of the as-milled $Cu_{50}Ti_{50}$ powders after the selected MA time. They all exhibit one distinct exothermic peak corresponding to the crystallization of the amorphous structure. The results suggest that the amorphous $Cu_{50}Ti_{50}$ powders were obtained after the milling time of 20 and 40 h. In the present work, the amorphous $Cu_{50}Ti_{50}$ powders after MA of 40 h were used for the dealloying process.

Fig. 2 shows the XRD patterns of the as-dealloyed samples obtained by dealloying the $Cu_{50}Ti_{50}$ amorphous powders in the HNO_3 solution for different durations. Several crystalline peaks identified as rutile TiO_2 are superimposed over a broad hump from the amorphous alloy when the corrosion time is 12 h. The cyrstalline phase is the rutile TiO_2, and the broad hump indicates the un-dealloyed amorphous alloy. It is clear that the phase transition occurs during the dealloying process of the amorphous $Cu_{50}Ti_{50}$ powders. The corrosion products after the immersion of 24 h are similar to those obtained at 12 h (the rutile TiO_2 and amorphous phase), as shown in Fig. 2. With increasing the immersion time from 24 to 36 h in the HNO_3 solution, the broad hump becomes weaker and the crystalline peaks become stronger, indicating that the amount of rutile TiO_2 phase increases in the as-dealloyed samples. It should be noted that further prolonging the dealloying

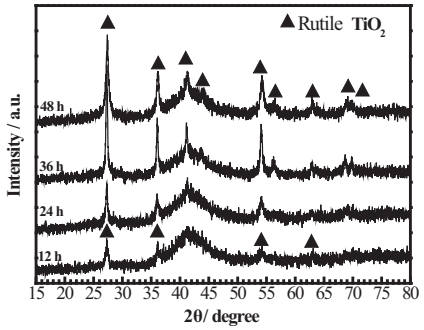

Fig. 2. XRD patterns of the as-dealloyed $Cu_{50}Ti_{50}$ samples subjected to the immersion in the HNO_3 solution for different durations.